

PHASE RELATIONS OF Mn-Fe-Si-C SYSTEMS

Eivind G. Hoel
Elkem Mangan KS Sauda, Norway

ABSTRACT

Phase relations of Mn-Fe-Si-C systems are established by means of reported binary diagrams, and calculations of ternary and quaternary diagrams. The phase relations are presented in diagrams for six binary and four higher order systems, the latter as liquidus surfaces and solid state equilibria at fixed temperature. Solidification progress of silicomanganese alloys are calculated, and the probable phase composition of solidified metal is predicted. The final phases appearing in silicomanganese alloys are $(\text{Mn,Fe})_5\text{Si}_3$, $(\text{Mn,Fe})_7\text{C}_3$ and $(\text{Mn,Fe})_3\text{Si}$ in MC SiMn, and $(\text{Mn,Fe})\text{Si}$, $(\text{Mn,Fe})_5\text{Si}_3$ and SiC in LC SiMn. In ferromanganese the phase $\alpha(\text{Mn,Fe})$ is present in all alloys, in addition to $(\text{Mn,Fe})_5\text{C}_2$ in HC FeMn, $(\text{Mn,Fe})_{23}\text{C}_6$ in MC and LC FeMn, and as the only phase in VLC FeMn.

INTRODUCTION

This presentation is a preliminary synopsis of parts of the author's doctoral work, a more comprehensive discussion and complementing information will be given in the doctoral thesis. The aim of the doctoral work is to establish the phase constitutions of commercial silicomanganese and some physical properties of the appearing phases. Results concerning silicomanganese alloys are in good agreement with experiments. The phase relations of ferromanganese alloys are obtained as a subsidiary to the work on silicomanganese, and are found convenient to include in this context, but are however *not* supported by experimental verifications by the author.

The doctoral work is carried out at the Norwegian Institute of Technology (NTH) dep. of Metallurgy and SINTEF dep. of Materials Technology, in Trondheim, Norway under the guidance of Prof. Johan Kr. Tuset, NTH and Sen. Research Scientist Ola Raanes, SINTEF. The research work is financially supported by The Norwegian Ferroalloy Producers Research Association (FFF) and The Research Council of Norway (NFR).

ACQUISITION OF THE DIAGRAMS

Phase relations of the Mn-Fe-Si-C system are established by means of reported binary diagrams, and calculations of ternary and quaternary diagrams. To obtain the most up to date phase relations, several reference works, textbooks and articles have been consulted. The diagrams presented are those agreed upon by the most recent sources. The ternary and quaternary diagrams in question have been difficult to obtain in the literature, although phase relations of minor parts are described in a number of articles. To acquire a complementary picture of the higher order phase relations, a computer program called 'Thermo-Calc' has been utilized.

Thermo-Calc is a general tool for thermodynamic calculations, developed at KTH in Stockholm, Sweden. Briefly explained this computer programme consists of a thermodynamic database, a calculation module and a user interface. The database contains descriptions of many binary and several higher order systems, and is updated and extended regularly. Thermo-Calc gives the user an opportunity to obtain thermodynamic data presented in various ways, not only limited to phase diagrams. Assumed the binary and preferably the ternary systems are described in the database, higher order systems can be calculated and the results obtained are experienced to be in good agreement with experimental data. It should be noticed that the database lacks descriptions necessary for calculations of ferroalloy slag systems. Diagrams obtained by Thermo-Calc are in this presentation identified by a triangular logo symbolizing a ternary phase diagram.

Main components of the ferroalloys in question are - in addition to iron - manganese and carbon in ferromanganese, in addition to silicon in silicomanganese. When produced from ordinary raw materials, several elements as Al, B, Ca, Mg, P, S, Ti and others are present. Quantities are usually low, less than 0.1 w% each, and they add up to about 0.5 w%. Common compositions of ferroalloys are given in table 1. Due to the low quantities, the influence of trace elements is neglected in this context. Hence, the binary and higher systems of importance are those given in table 2.

BINARY SYSTEMS

The binary systems according to the given references are shown in figure 1 to 6. The complexity of these systems varies a lot, from the simple silicon-carbon system with only one intermediate compound, to the complex systems of manganese-silicon and manganese-carbon. From the binary systems presented, it is obvious that many phases can occur, the most important of these are given in table 3, along with their region of appearance. The given ranges includes both the one-phase region and regions of coexistence with other phases.

The binary systems used for the Thermo-Calc database are generally in very good agreement with the diagrams presented here. There are minor differences in temperature and composition of some invariant reactions, where the actual values are disputed. This mainly affects solid state reactions, e.g. in the manganese-carbon system. Compounds with narrow solubility regions are simplified and considered as stoichiometric phases, e.g. in the manganese-silicon system. Some reported compounds are not included, due to uncertainty of their existence in the pure binary system.

Table 1: Ferroalloy compositions.

Typical values, main elements varies within alloy specification.

Alloy	weight percent					atomic percent ²			
	Fe	Si	Mn	C	X ¹	Fe	Si	Mn	C
<i>Ferromanganese</i>									
HC FeMn	13.5	0.2	79	7.0	0.5	11	0.8	63	26
MC FeMn	16.5	0.5	81	1.5	0.5	16	0.4	77	6.5
LC FeMn	17	0.3	82	0.5	0.5	17	0.2	81	2.2
VLC FeMn	19	0.3	80	0.1	0.5	21	0.2	79	0.5
<i>Silicomanganese</i>									
MC SiMn	10	19	69	1.5	0.5	8	29	57	5.6
LC SiMn	9.5	29	61	0.1	0.5	7	45	47	0.4

¹Trace elements: Al, B, Ca, Mg, P, S, Ti and others, <0.1 w% each.

²Trace elements excluded from calculation.

Table 2: Binary and higher systems of importance to ferroalloys.

Alloy	Binary	Higher
<i>Ferromanganese</i>	Fe-Mn Fe-C Mn-C	Mn-Fe-C
<i>Silicomanganese</i> ¹	Fe-Si Mn-Si Si-C	Mn-Fe-Si Mn-C-Si Mn-Fe-C-Si

¹In addition to those of ferromanganese.

HIGHER ORDER SYSTEMS

Calculated ternary and quaternary diagrams are in good agreement with reported observations. Minor differences are detected, but not discussed here. This should nevertheless be noted if using the diagrams.

Manganese-iron-carbon

The ternary system manganese-iron-carbon is shown in figure 7 and 8. It is cut at 50 a% C due to little interest of higher carbon contents. The liquidus surface falls steeply from the very high temperatures in the C-rich part of the diagram. Graphite is the primary phase above ~25 a% C. $\gamma(\text{Mn,Fe})$ is in equilibrium with the melt from the Mn-Fe baseline up to ~10 a% C at the manganese apex and up to ~20 a% C at the iron apex. In the intermediate triangle several phases coexist with the melt. Mn_7C_3 and ϵ extend from the Mn-C side. Mn_5C_2 and Fe_3C are present within regions at ~30 a% Fe/20 a% Si and ~50 a% Fe/18 a% Si, respectively. $\gamma(\text{Mn,Fe})$ and Fe_3C forms the lowest melting point, at 1076 °C and 56 a% Fe/16 a% C. Minor existence regions of δMn and δFe are left out due to little importance.

At the isothermal cross section in solid state at 800 °C, ϵ has disappeared, while four new phases appear, Mn_{23}C_6 , βMn , αMn and αFe . Manganese and iron are, in varying extent, substituted by each other in all the metal-carbon compounds, $\gamma(\text{Mn,Fe})$ is continuous from 0 to 100 a% Fe. Due to the extended formation of solid solutions this system is dominated by large areas of two-phase equilibria.

The cross section at Mn:Fe-ratio 7:1 differs very little from the pure Mn-C system.

Manganese-iron-silicon

The ternary system manganese-iron-silicon is shown in figure 9 and 10. The liquidus surface is divided at 50 a% Si by the continuous ridge of $(\text{Mn,Fe})\text{Si}$. In the Si-rich part the two phases $(\text{Mn,Fe})\text{Si}$ and Si are the dominating primary phases. Within a small intermediate region at ~70 a% Si, $\text{FeSi}_{2,h}$ and $\text{Mn}_{11}\text{Si}_{19}$ appear at the liquidus surface. The lowest melting point of this part is the eutectic between Si, $\text{Mn}_{11}\text{Si}_{19}$ and MnSi, at 1136 °C and 2 a% Fe/67 a% Si. At lower Si-concentrations

Table 3: Significant phases of binary systems.

System Phase	Range of existence	
	atomic%	temp. [°C]
<i>Manganese-Iron</i>		
$\gamma(\text{Mn,Fe})$	0-100	-1473°
βMn	0-38	700-1155°
αMn	0-47	-707°
<i>Manganese-Silicon</i>		
βMn	0-18.7	-1155°
Mn_9Si_2	16.7-21	-1060°
Mn_3Si	21-37.5	-1075°
Mn_5Si_3	24-46	-1285°
MnSi	46-64.5	-1275°
$\text{Mn}_{11}\text{Si}_{19}$	50-100	-1155°
Si	63-100	-1414°
<i>Iron-Silicon</i>		
$\alpha\delta\text{Fe}$	0--20	-1538°
Fe_3Si	11-32	-1234°
Fe_2Si	32-36	1040-1212°
FeSi	36-67	-1410°
$\text{FeSi}_{2,h}$	50-100	937-1220°
$\text{FeSi}_{2,l}$	50-100	-982°
Si	67-100	-1414°
<i>Manganese-Carbon</i>		
γMn	0-20.7	770-1243°
αMn	0-20.7	-818°
ϵ	10.5-30	990-1308°
Mn_{23}C_6	6.5-28.6	-1034°
Mn_5C_2	21.8-30	-1171°
Mn_7C_3	22.9-100	-1333°
graphite	26.7-100	->2000°
<i>Iron-Carbon (metastable: italicized)</i>		
γFe	0-17	-730-1493°
αFe	0-25/100	--730°
Fe_3C	0-100	-1252°
graphite	0/25-100	->2000°
<i>Silicon-Carbon</i>		
Si	0-50	-1414°
SiC	0-100	-2545°

a number of phases coexist with the melt. The manganese compounds, Mn_5Si_3 , Mn_3Si and βMn , all extend towards high iron contents. At the Mn-Fe baseline $\gamma(Mn,Fe)$ exists within a large region, and $\alpha\delta Fe$ in a minor area extending towards the Fe-Si side. The last iron compound, Fe_2Si , is present within a small area at ~33 a% Si. The lowest melting point of the entire system is the eutectic between Mn_3Si , βMn and $\gamma(Mn,Fe)$, at 1015 °C and 45 a% Fe/20 a% Si. Minor existence regions of δMn and Mn_9Si_2 are left out due to little importance.

At the isothermal cross section in solid state at 800 °C, Fe_2Si has disappeared, $FeSi_2$ is transformed to its low temperature modification, while one new phase appears, Mn_6Si . An important feature of this system is the continuous solid solutions of the metal-silicon compounds, $(Mn,Fe)Si$, $(Mn,Fe)_5Si_3$ and $(Mn,Fe)_3Si$. As in the Mn-Fe-C system manganese and iron are substituting each other. In this system the Si-rich part consists mainly of three-phase regions, the middle part of two-phase regions and the Mn/Fe-rich part of one-phase regions.

The cross section at Mn:Fe-ratio 7:1 differs in minor degree from the pure Mn-Si system, it is however simplified by the disappearance of the two phases Mn_9Si_2 and Mn_6Si .

Manganese-carbon-silicon

The most important part of the ternary system manganese-carbon-silicon is shown in figure 11 and 12. As seen the liquidus surface falls steeply from the very high temperatures in the C-rich part of the diagram. Graphite is the primary phase above ~25 a% C at the Mn-C baseline, and this region extends up the C/SiC coexistence line at ~13 a% C. SiC is present from ~21 a% Si and extends towards the Mn-Si side, above ~45 a% Si only a tiny strip is left for other phases. In the Mn-rich part several phases coexist with the melt. From the Mn-C baseline γMn , ϵ , and Mn_7C_3 extend above ~20 a% Si. Mn_5C_2 is present within a narrow area at ~8 a% C/17 a% Si. At the Mn-Si side βMn and $MnSi$ is present within narrow areas, while Mn_3Si and Mn_5Si_3 extend towards ~5 and ~11 a% C, respectively. The lowest melting point is the eutectic between Mn_3Si , βMn and γMn , at 1014 °C and 2 a% C/19 a% Si. Minor existence regions of δMn and Mn_9Si_2 are left out due to little importance.

At the isothermal cross section in solid state at 800 °C, two new phases appears, Mn_6Si and $Mn_{23}C_6$. Binary compounds do not take the third component into solid solutions, except for the narrow ranges of βMn and γMn , where limited solid solutions are formed. Thus, in this system there are mainly three-phase equilibrium regions. Only at the Mn apex small two- and one-phase regions occurs.

Manganese-iron-carbon-silicon

As stated earlier it is necessary to fix the ratio of two components of a quaternary system. The previous discussions of the binary and ternary systems, shows that manganese is substituted by iron in most phases. At low concentrations of iron, manganese and iron can be considered as one component. It is thus convenient to fix this ratio, according to table 1 the Mn:Fe-ratio in silico-manganese is ~7:1. The quaternary system is therefore represented by the pseudo ternary system Mn7Fe-carbon-silicon, as shown in figure 13 and 14, where the most interesting parts are given. Phases named MnX are consisting both Mn and Fe, and should be read (Mn,Fe)X. The Mn:Fe-ratio is usually ~7:1, but smaller deviations from this may occur.

The liquidus surface is similar to that for the pure Mn-C-Si system. Identical phases occur, but most boundary lines are shifted towards the Mn7Fe apex. This tendency is evident for the graphite/Mn₇C₃ and SiC/Mn₅Si₃ coexistence lines, and the boundaries of Mn₅C₂. This compound is present within a larger area and extends to the Mn7Fe-C baseline. The lowest melting point is the eutectic between Mn₃Si, βMn and γMn, at 1000 °C and 3 a% C/18 a% Si. A minor existence region of δMn is left out due to little importance.

At the isothermal cross section in solid state at 800 °C, one new phase appears, Mn₂₃C₆. Compared to the pure Mn-C-Si system, some differences are apparent. Two phases are not present, Mn₉Si₂ and Mn₆Si.

PHASES OF FERROALLOYS

Phase diagrams can be used to establish the solidification paths of the alloys, and from these be able to predict which phases are formed from the liquid. There is however a very important limitation. The phase diagrams are, by definition, equilibrium diagrams, and no information are given about the reaction kinetics. As seen from the presented diagrams, transformations in solid state frequently occur. These reactions are slow, compared to reactions at the liquidus. Casting at industrial scale often gives fast solidification and cooling, away from equilibrium conditions. Thus, the actual phases formed in a solidified alloy may deviate quite considerably from the predicted ones. It should from this be understood that a determination of the phase relations of ferroalloys is not simple.

Predictions concerning silicomanganese alloys are in good agreement with experimental results, although these are not discussed here. The predicted phase relations of ferromanganese alloys are however *not* supported by experimental verifications by the author.

Ferromanganese

Ferromanganese alloy compositions and probable solidification progress are shown in figure 15, supplementary data are given in table 4. HC FeMn liquid coexists with graphite above 1306 °C, where the saturation concentration is ~25 a% C. The solidification path starts within the phase field of graphite, somewhat above the C/Mn₇C₃ coexistence line, and is directed towards this line. Excess carbon from the supersaturated melt is thus precipitated as graphite, which floats to the top of the melt, due to the low density, 2.22 g/cm³, compared to ~7 g/cm³ of the melt. Graphite is assumed not to take part in any reactions in the continuation. The formation of the primary phase Mn₇C₃ takes place below 1306 °C, and the solidification path continues through the phase fields of Mn₇C₃ and Mn₅C₂, follows the Mn₅C₂/ε, ε/Fe₃C and Fe₃C/γ(Mn,Fe) coexistence lines, passing several peritectica.

Table 4: Phases of ferroalloys. Carbon saturation.

Alloy	Solid state phases	C _{sat} -equilibrium	C _{sat} a%/w%
HC FeMn	α(Mn,Fe), Mn ₅ C ₂ , graphite ¹	graphite/Mn ₇ C ₃	24.7 6.7
MC FeMn	α(Mn,Fe), Mn ₂₃ C ₆	-	- -
LC FeMn	α(Mn,Fe), Mn ₂₃ C ₆	-	- -
VLC FeMn	α(Mn,Fe)	-	- -
MC SiMn	Mn ₅ Si ₃ , Mn ₇ C ₃ , Mn ₃ Si, SiC ¹	SiC/Mn ₅ Si ₃	3.4 0.9
LC SiMn	MnSi, Mn ₅ Si ₃ , SiC	SiC/MnSi	0.4 0.1

¹Segregated precipitate from supersaturated melt.

The many Mn-C compounds present in this region make it difficult to determine the final situation. Suggested solid state reactions eliminate the primary phases of Mn_7C_3 , ϵ and Fe_3C , and include $\gamma(Mn,Fe)$ transformation to $\alpha(Mn,Fe)$. According to this the final phases present are $\alpha(Mn,Fe)$ and Mn_5C_2 , in addition to segregated graphite.

The solidification paths of the other FeMn alloys, i.e. MC, LC and VLC are simpler. The liquid alloys are, due to the MOR-treatment, not saturated with carbon. The only primary phase formed from the liquid of these alloys is $\gamma(Mn,Fe)$, and the only probable solid state reaction is the $\gamma(Mn,Fe)$ transformation to $\alpha(Mn,Fe)$, in MC and LC FeMn accompanied by precipitation of $Mn_{23}C_6$. The final phases are accordingly $\alpha(Mn,Fe)$ and $Mn_{23}C_6$ in MC and LC, and $\alpha(Mn,Fe)$ only, in VLC FeMn.

Silicomanganese

Silicomanganese alloy compositions and probable solidification progress are shown in figure 16, supplementary data are given in table 4. MC SiMn liquid coexists with SiC above 1224 °C, where the saturation concentration is 3.4 a% C. The solidification path starts within the phase field of SiC, and is directed towards the SiC/ Mn_5Si_3 coexistence line. Excess carbon from the super-saturated melt is thus precipitated as SiC, which floats to the top of the melt, due to the low density, 3.22 g/cm³, compared to ~6 g/cm³ of the melt. SiC is assumed not to take part in any reactions in the continuation. The formation of the primary phase Mn_5Si_3 takes place below 1224 °C, and the solidification path continues through the phase field of Mn_5Si_3 , follows the Mn_5Si_3/Mn_7C_3 coexistence line, and ends at the $Mn_5Si_3/Mn_7C_3/Mn_3Si$ peritecticum. No solid state reactions takes place. The final phases are consequently Mn_5Si_3 , Mn_7C_3 and Mn_3Si , in addition to segregated SiC.

LC SiMn liquid coexists with SiC above 1264 °C, where the saturation concentration is 0.4 a% C. Primary phase is MnSi. The solidification path follows the SiC/MnSi coexistence line, and ends at the MnSi/ Mn_5Si_3 /SiC peritecticum. No solid state reactions takes place. The final phases are accordingly MnSi, Mn_5Si_3 and SiC.

REFERENCES

- [1] Kubashewski, Ortrud: *Iron Binary Phase Diagrams*, Springer-Verlag, 1982.
- [2] Shunk, F. A.: *Constitution of Binary Alloys, 2. supplement*, McGraw-Hill, 1969.
- [3] Massalski, T. B.: *Binary Alloy Phase Diagrams, 2. edition*, ASM International, 1990.
- [4] Huang, W.: *Thermodynamic Assessment of the Mn-C System*, Scan. J. Met., 19, 26, 1990.
- [5] Scace, R. I.: *Solubility of Carbon and in Silicon and Germanium*, J. Chem. Phys., 30, 1551, 1959.
- [6] Dolloff, R. T.: *Silicon-Carbon Binary System in Research Study to Determine the Phase Equilibrium Relations of Selected Metal Carbides at High Temperatures*, WADD Tech. Rep., 60-143, 1960.

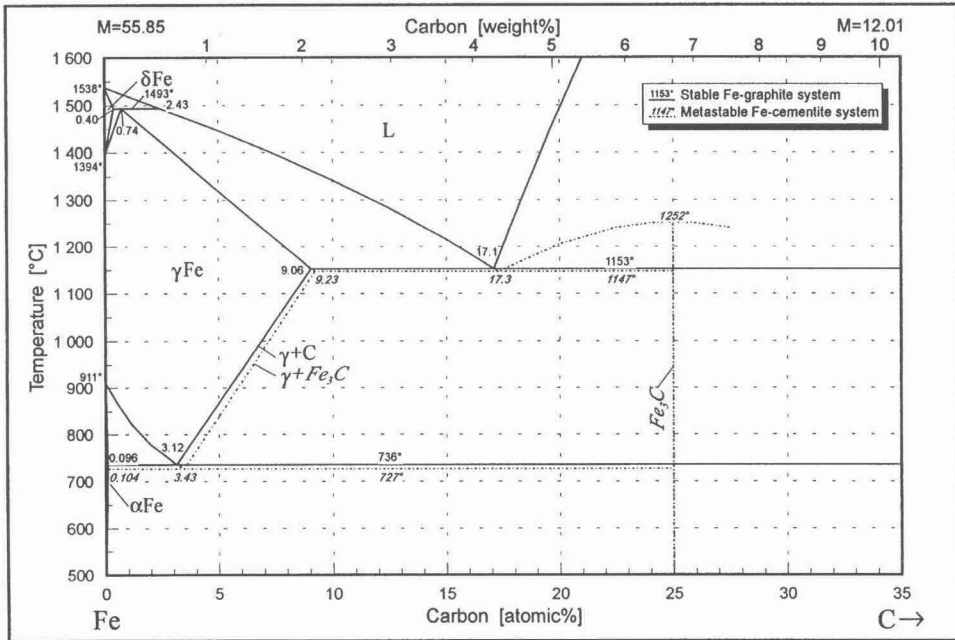


Figure 5: The binary system iron-carbon. After [1].

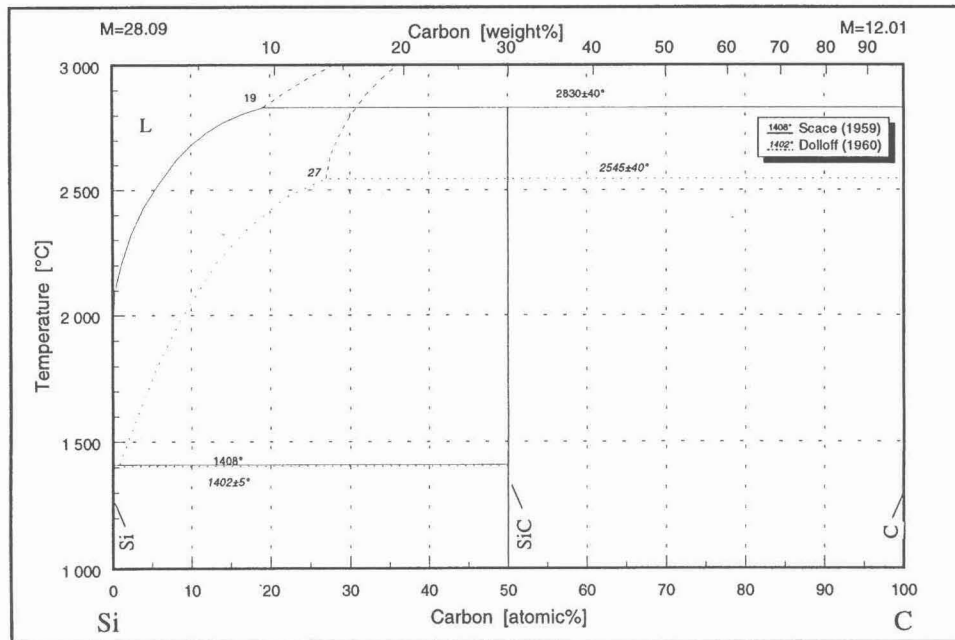


Figure 6: The binary system silicon-carbon. After [5], [6].

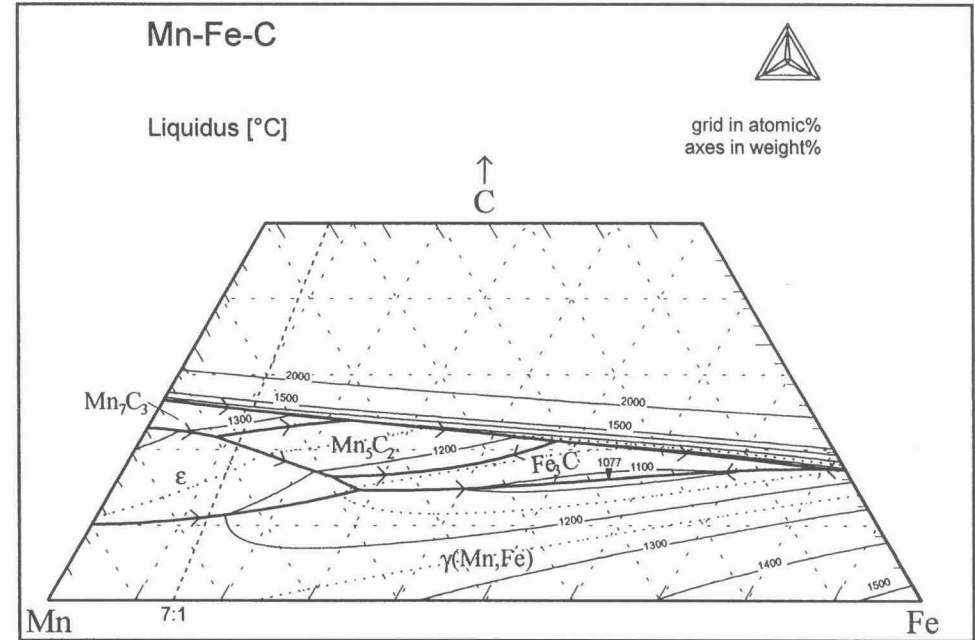


Figure 7: The ternary system manganese-iron-carbon, liquidus surface.

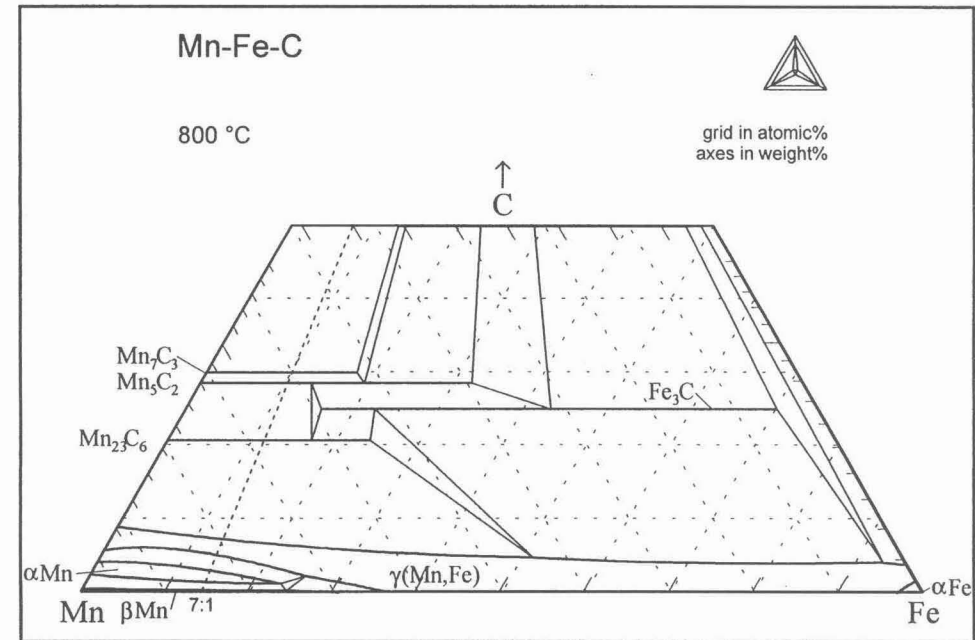


Figure 8: Manganese-iron-carbon, isothermal cross section at 800 °C.

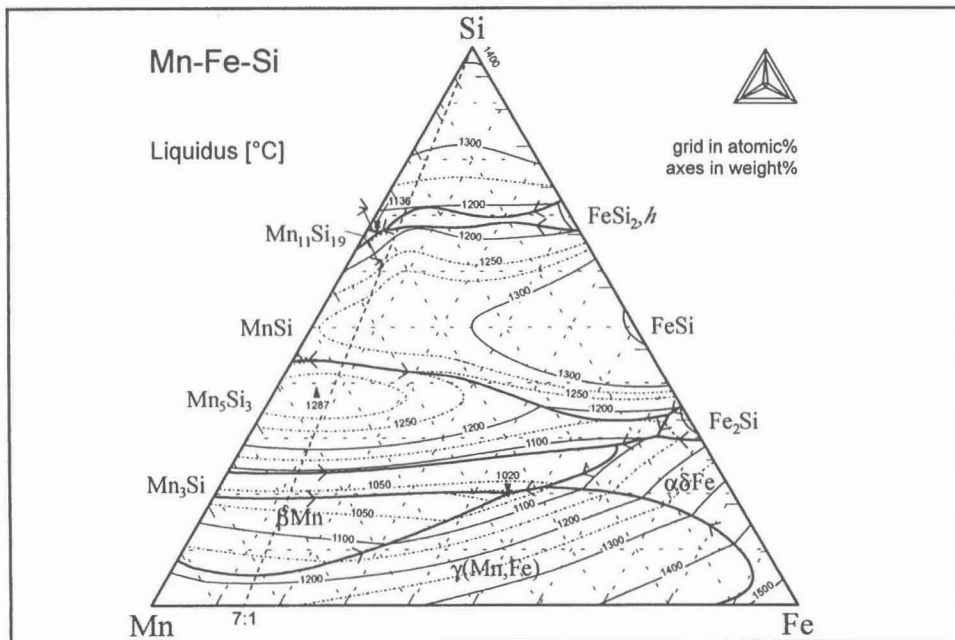


Figure 9: The ternary system manganese-iron-silicon, liquidus surface.

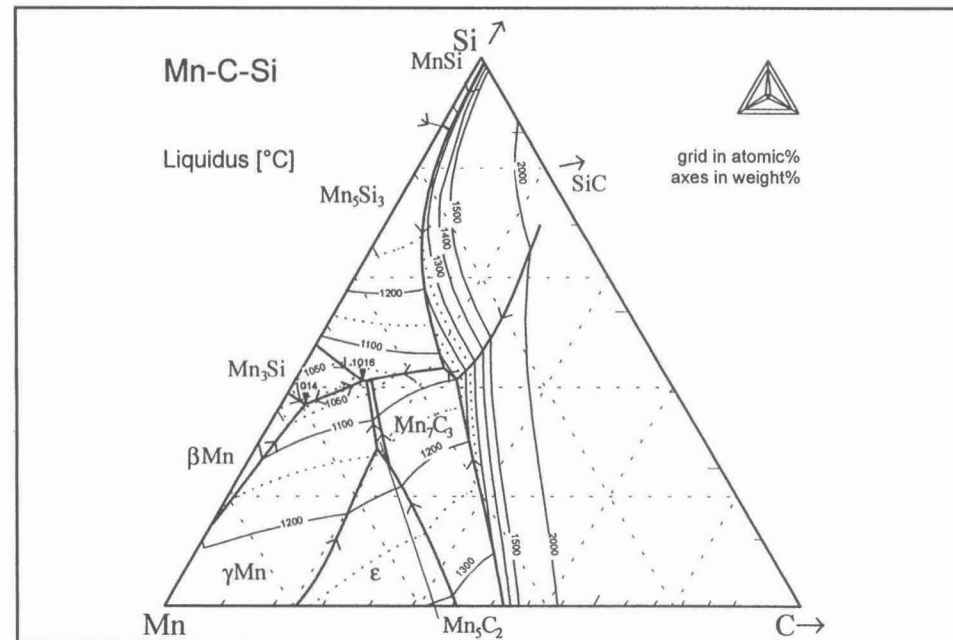


Figure 11: The ternary system manganese-carbon-silicon, liquidus surface.

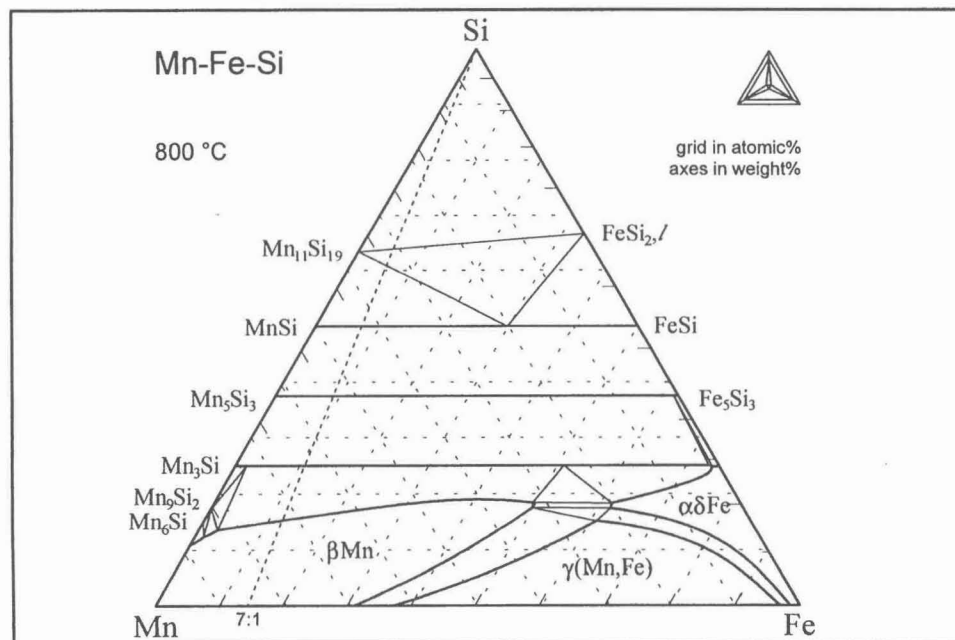


Figure 10: Manganese-iron-silicon, isothermal cross section at 800 °C.

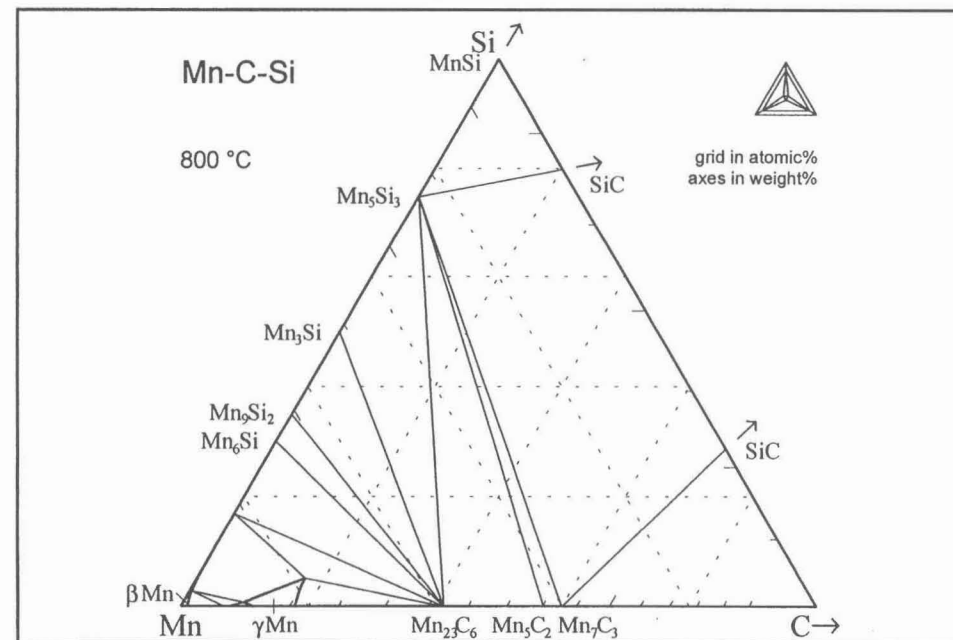


Figure 12: Manganese-carbon-silicon, isothermal cross section at 800 °C.

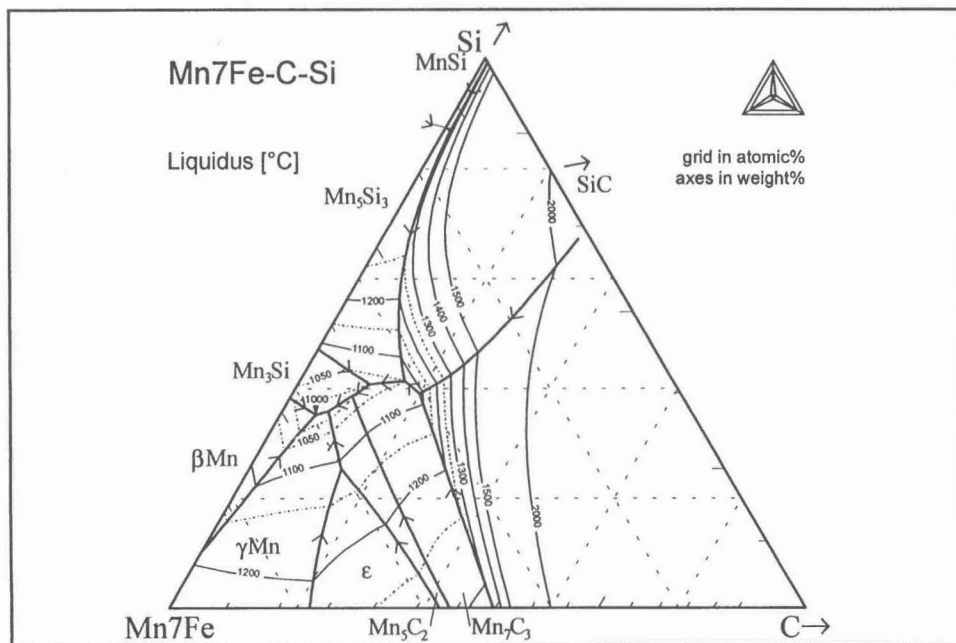


Figure 13: The system Mn7Fe-carbon-silicon, liquidus surface.

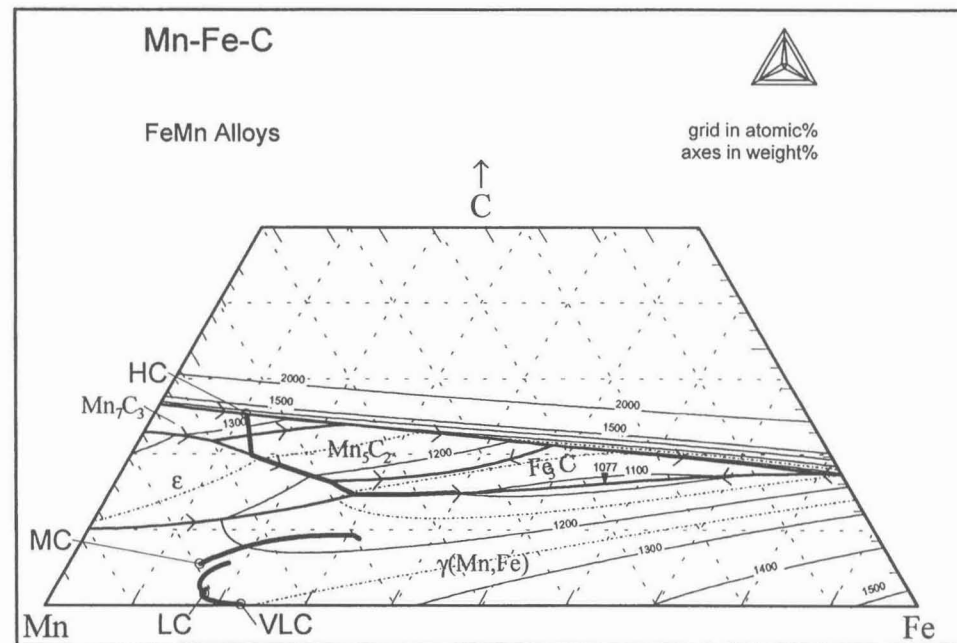


Figure 15: FeMn alloy compositions and probable solidification paths.

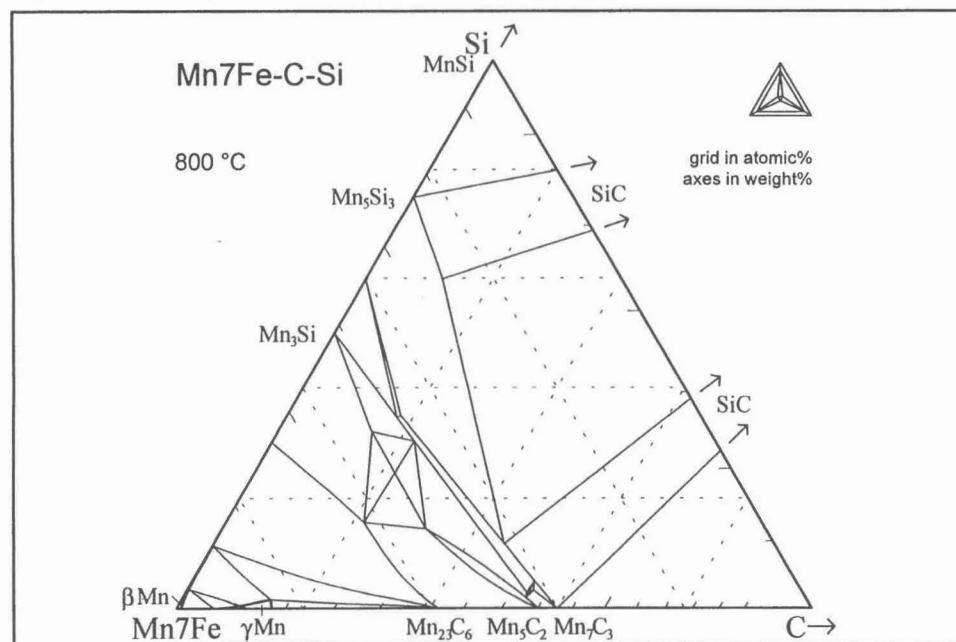


Figure 14: Mn7Fe-carbon-silicon, isothermal cross section at 800 °C.

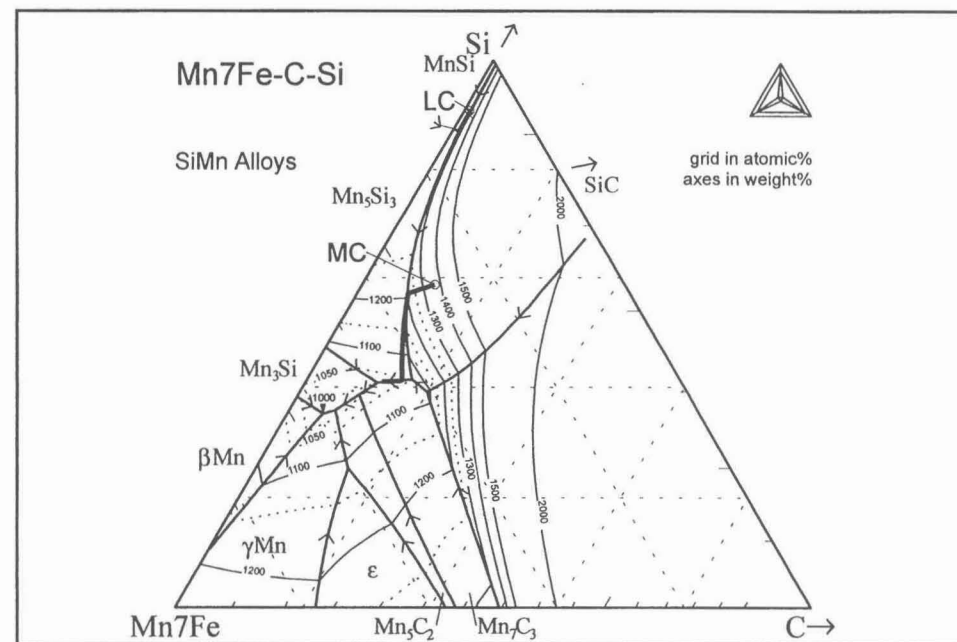


Figure 16: SiMn alloy compositions and probable solidification paths.